

AD-A141 562

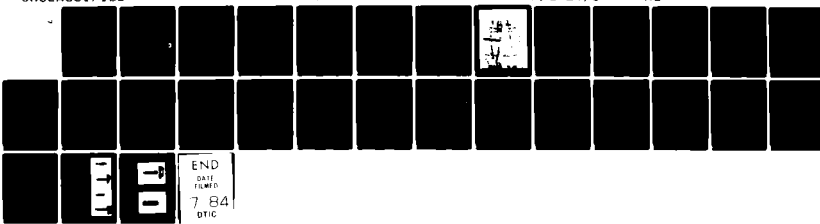
HIGH SPEED EJECTORS(U) FLIGHT DYNAMICS RESEARCH CORP
VAN NUYS CALIF M ALPERIN 04 APR 84 AFOSR-TR-84-0430
F49620-81-C-0043

1/1

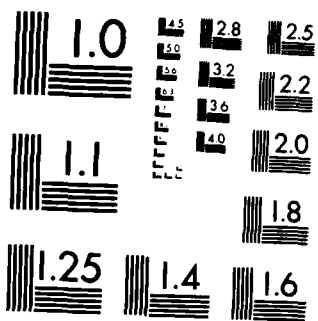
UNCLASSIFIED

F/G 21/5

NL



END
DATE FILMED
7-84
DTIC



MICROCOPY RESOLUTION TEST CHART
NATIONAL BUREAU OF STANDARDS 1963-A

UNCLASSIFIED

AD-A141 562

SECURITY CLASSIFICATION OF THIS PAGE

REPORT DOCUMENTATION PAGE			
1a. REPORT SECURITY CLASSIFICATION UNCLASSIFIED	1b. RESTRICTIVE MARKINGS		
2a. SECURITY CLASSIFICATION AUTHORITY	3. DISTRIBUTION/AVAILABILITY OF REPORT Approved for Public Release; Distribution Unlimited.		
2b. DECLASSIFICATION/DOWNGRADING SCHEDULE			
4 PERFORMING ORGANIZATION REPORT NUMBER(S) 8F161	5. MONITORING ORGANIZATION REPORT NUMBER(S) AFOSR-TR-84-0430		
6a. NAME OF PERFORMING ORGANIZATION Flight Dynamics Research Corp.	6b. OFFICE SYMBOL (If applicable)	7a. NAME OF MONITORING ORGANIZATION <i>AFOSR/NA</i>	
6c. ADDRESS (City, State and ZIP Code) 15809 Stagg Street Van Nuys, California 91406	7b. ADDRESS (City, State and ZIP Code) <i>Bolling AFB, DC 20332</i>		
8a. NAME OF FUNDING/SPONSORING ORGANIZATION AIR FORCE OFFICE OF SCIENTIFIC RESEARCH	8b. OFFICE SYMBOL (If applicable) AFOSR/NA	9. PROCUREMENT INSTRUMENT IDENTIFICATION NUMBER F49620-81-C-0043	
10. SOURCE OF FUNDING NOS. PROGRAM ELEMENT NO. 61102F	PROJECT NO. 2307	TASK NO. A1	WORK UNIT NO.
11. TITLE (Include Security Classification) High Speed Ejectors (UNCL)	12. PERSONAL AUTHORIS. Alperin, Morton		
13a. TYPE OF REPORT Annual	13b. TIME COVERED FROM 82/22/3 TO 84/31/3	14. DATE OF REPORT (Yr., Mo., Day) 84/4/4	15. PAGE COUNT 29
16. SUPPLEMENTARY NOTATION <i>DTIC SELECTED MAY 30 1984 A</i>			
17. COSATI CODES FIELD GROUP SUB GR.	18. SUBJECT TERMS (Continue on reverse if necessary and identify by block number) High Speed Ejectors		
19. ABSTRACT (Continue on reverse if necessary and identify by block number) A description of the test apparatus and some major experimental results are presented. The test apparatus is a pressurized test cell for simulation of translational motion by pressurization of the inlet flow to the corresponding stagnation pressure. The experiment consisted of measurement of the pressure distribution along the ejector surfaces and critical pressure, temperature and forces required to evaluate the mass flow, total forces and drag. In addition, Schlieren photographs were taken at each test to observe the flow and in particular to illustrate the shock wave patterns. Combination of the pressure distribution and Schlieren photographs illustrate the successful achievement of secondary solution flows. Further tests are to be performed to illustrate the optimization of secondary solution performance and for comparison between theory and experiment.			
20. DISTRIBUTION/AVAILABILITY OF ABSTRACT UNCLASSIFIED/UNLIMITED <input checked="" type="checkbox"/> SAME AS RPT <input type="checkbox"/> DTIC USERS <input type="checkbox"/>		21. ABSTRACT SECURITY CLASSIFICATION UNCLASSIFIED	
22a. NAME OF RESPONSIBLE INDIVIDUAL Dr. James Wilson		22b. TELETYPE NUMBER (Include Site Code) (202) 767-4035	22c. OFFICE SYMBOL AFOSR/NA

FDRC/DOE/DOE
N-1 GRAB
TAB
U.S. GOVERNMENT



Flight Dynamics Research Corporation
Annual Report - High Speed Ejector
Contract No. F49620-81-C-0043
April 1984

A-1

Research Objective

The ejector component models and their test set-up have been designed to provide measurement of the pressure distributions along the upper and lower surfaces of the ejector at various outlet area ratios and to measure the forces, and primary and secondary pressures and temperatures required to evaluate the mass flows and thrust augmentations at various ejector geometries and simulated flight conditions.

Status of the Research Effort

Test Set-up

The FDRC static test stand has been modified to accept the ejector model as illustrated on Figure 1. The primary, high pressure, ambient temperature air is supplied from a pressure vessel having a maximum pressure of 250 psig. The discharge from the pressure vessel is controlled by a remote valve and pressure regulator, through an orifice, to permit a controlled, adjustable pressure at the primary nozzles. To simulate the stagnation pressure due to translational flight, the secondary air is supplied from a Model RAS 60, 717 Roots Connersville displacement blower, through a system of tubes, orifices and valves. Its pressure is controlled by the use of a by-pass system permitting secondary air stagnation pressures to about 8 psig, simulating a flight Mach number of about 0.8.

The ejector is enclosed in a box capable of maintaining the secondary air and fitted with adjustable primary nozzles. The ejector component has a width of 3.0 inches and a height which has been varied from 0.25 inches to 1.0 inches, and a mixing length which can be varied from about 1.0 inches to about 3.5 inches. The outlet of the 1.0 inch ejector is remotely adjustable to provide a means for starting the second solution flow and for achieving the outlet area required for efficient operation of the second solution flow.

Approved for public release;
distribution unlimited.

84 05 29 095

Test results

Table I is a summary of the tests performed on various ejectors having fixed and/or variable outlet geometries and variable primary pressures.

TABLE I

Config	Throat width	Outlet width	Mixing length	Flight Mach No.	Remarks
α_*	x_2	x_E	z_m	M_∞	
7.55	0.25	0.25	2.5	0.5	DN
7.55	0.25	0.25	2.5	0.65	DN
7.55	0.25	0.25	2.5	0.81	DN
7.55	0.25	0.212	2.5	0.65	DN
7.55	0.25	0.212	2.5	0.81	DN
15.1	0.501	0.443	2.5	0.65	DN
15.1	0.501	0.443	2.5	0.81	DN
30.2	0.986	0.883	1.5	0.65	DN
30.2	1.000	0.906	2.5	0.5	DN
30.2	1.000	0.906	2.5	0.65	DN
30.2	1.000	0.906	2.5	0.81	DN
30.2	1.000	0.906	3.5	0.65	DN
30.2	1.000	0.906	3.5	0.81	DN
15.1	0.25	0.22	2.5	0.65	SCN $z_p = -.25$
15.1	0.25	0.22	2.5	0.81	SCN $z_p = -.25$
15.1	0.25	0.22	2.5	0.81	SCN $z_p = -.75$
30.2	0.501	0.44	2.5	0.65	SCN $z_p = -.25$
30.2	1.000	0.9-1.3	2.5	0.5	DN
30.2	1.000	0.9-1.3	2.5	0.65	DN
30.2	1.000	0.9-1.3	2.5	0.81	DN

DN - double array of nozzles

SCN - single array of central nozzles

z_p - position of primary nozzles relative to entrance to mixing section

AIR FORCE INSTITUTE OF SCIENTIFIC RESEARCH (AFSC)
 NOTICE OF APPROVAL TO PUBLISH
 This report has been approved for publication by AFSC
 APPROVED FOR PUBLIC RELEASE BY AFSC
 DISTRIBUTION STATEMENT A: AFSC-12.
 MATTHEW J. KELLY
 Chief, Technical Information Division

Pressure distributions along the ejector surfaces are presented on Figures 2 through 21.

Figure 2 illustrates the pressure distribution along the ejector surfaces at a simulated Mach number of 0.5 for the smallest ejector tested. As can be observed on Figure 2, the sharp pressure rise in the constant cross-section mixing section occurs at a primary plenum pressure (P_{op}) of about 65.3 psig, and proceeds downstream as the primary plenum pressure is increased. As shown on Figure 22, that rapid rise of pressure is a result of the presence of a starting shock wave. At a primary plenum pressure of 70.5 psig, the Schlieren photograph presented on Fig. 22 indicates the presence of a shock wave at about the center of the mixing section. As the primary plenum pressure is further increased, the shock wave progresses towards the exit of the ejector and reaches the end of the uniform cross-section at a plenum pressure of 85.1 psig.

Figure 3 illustrates the pressure distribution for the same ejector at a simulated flight Mach number of 0.65. At this increased flight Mach number the shock wave is able to exit the ejector and to form a system of oblique shock waves outside of the ejector, as shown for primary plenum pressures in excess of 80.3 psig. This is further corroborated by observation of Fig. 23, which depicts the external oblique system of shock waves. Thus it may be concluded that the ejector flow represents a second solution flow in a constant cross-section ejector.

The efficient operation of a second solution ejector requires a correct outlet configuration. Thus the geometry illustrated on Fig's 2 - 4 represents the achievement of a second solution ejector flow, however it is not efficient, since the outlet area ratio is not optimized, as described in Ref's 1 and 2. Further attempts to achieve second solution flows with ejectors having fixed outlets with area ratios less than 1.0 did not result in second solution flows, as illustrated on Figures 5 - 18.

Figures 5 - 18 depict pressure distributions of ejectors having outlet configurations theoretically designed for starting a second solution flow. However, these ejector outlets are within the one-dimensional geometric limitations of the first solution outlet designs, and therefore they default to the first solution, as explained in Ref. 3.

Further testing of the variable outlet ejector resulted in the pressure distributions illustrated on Fig's. 19 - 21. The results indicate that for those simulated flight Mach numbers and for outlet configurations which were not within the limitation of the first solution (X_e/X_2 greater than the first solution limit) the second solution flow was achieved. Thus as indicated on the Schlieren photograph of Fig 24, for $\alpha_* = 30.2$, $M_\infty = 0.81$, and $X_e/X_2 = 1.1$, at a primary plenum pressure of 75 psig, (an outlet area ratio which is greater than that prescribed for the limit of the first solution) the second solution has been achieved, since the shock wave can be observed in the diverging supersonic nozzle.

To achieve the desired goal of an efficient high speed ejector, it is intended to test the variable outlet ejector and to reduce the outlet area after starting the second solution flow at a larger outlet area. To perform those tests it is important to recalibrate the test rig and instrumentation, since the measurement of thrust augmentation on the present static test rig requires high accuracy in measurement of the pressures, temperatures and forces.

References

1. Alperin, M. and Wu J.J., "Thrust Augmenting Ejectors, Part I," AIAA Journal, Vol. 21, Oct 1983, pp 1428-1436.
2. Alperin, M. and Wu J.J., "Thrust Augmenting Ejectors, Part II," AIAA Journal, Vol. 21, Dec 1983, pp 1698-1706.
3. Alperin, M. and Wu J.J., "Remarks on Fabri and Siestrunk Supersonic Air Ejectors," to be published.

Publications

The papers published in technical journals are those listed as Ref's 1 & 2. A third paper (Ref. 3) has been presented to the AIAA Journal for publication and is presently being reviewed.

Personnel

Dr. Morton Alperin, Ph.D. 1950 Cal. Inst. of Tech.
Mr. Jiunn-Jenq Wu, Eng. 1971 Cal. Inst. of Tech.
Ms. Marilyn Stein, BS 1983 Univ. of Cal. Los Angeles

Interactions

A paper has been presented at the Ejector Workshop for Aerospace Applications at the University of Dayton, June 1982.

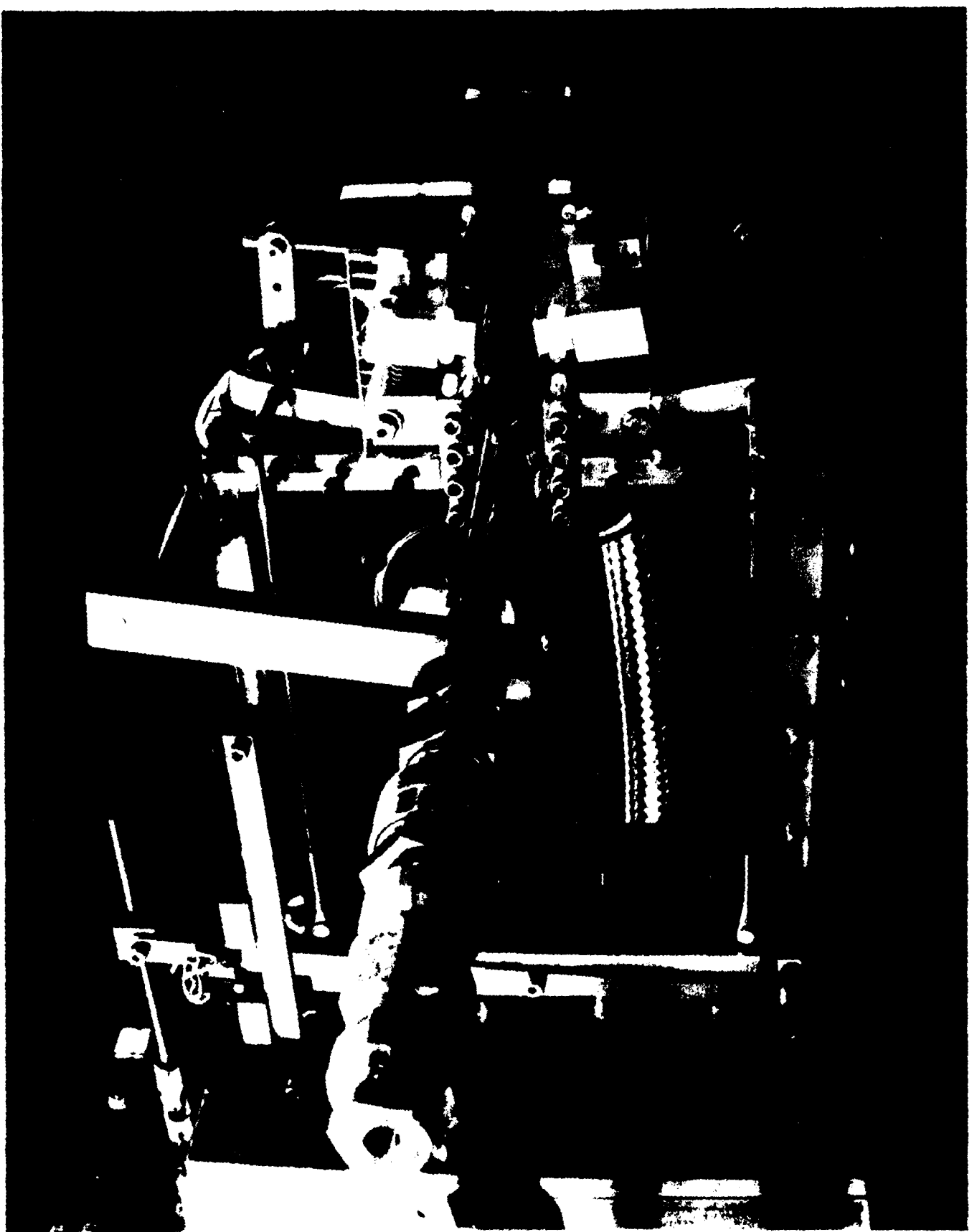


Figure 1. High Speed Ejector - Test Apparatus

$\alpha_0 = 7.55$
 $M_\infty = 0.5$
 $(P_{\infty} = 2.74 \text{ psig})$
 $x_2 = 0.250 \text{ inch}$
 $x_c = 0.250 \text{ inch}$
 $z_m = 2.5 \text{ inch}$
Primary Nozzles:
 $\theta_p = 10^\circ$
 $z_p = -0.554 \text{ inch}$
 $x_p = 0.126 \text{ inch}$

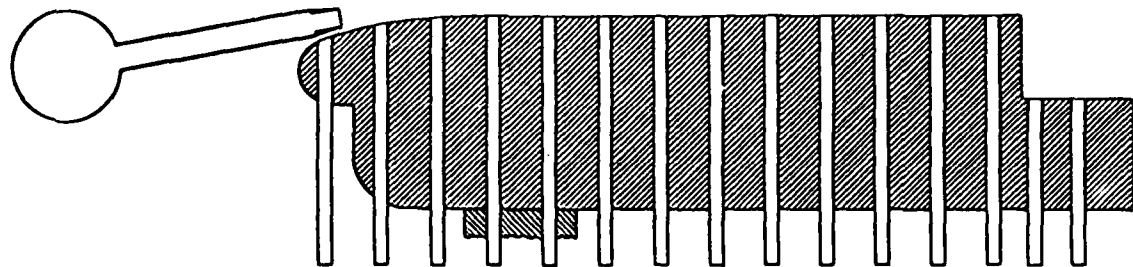
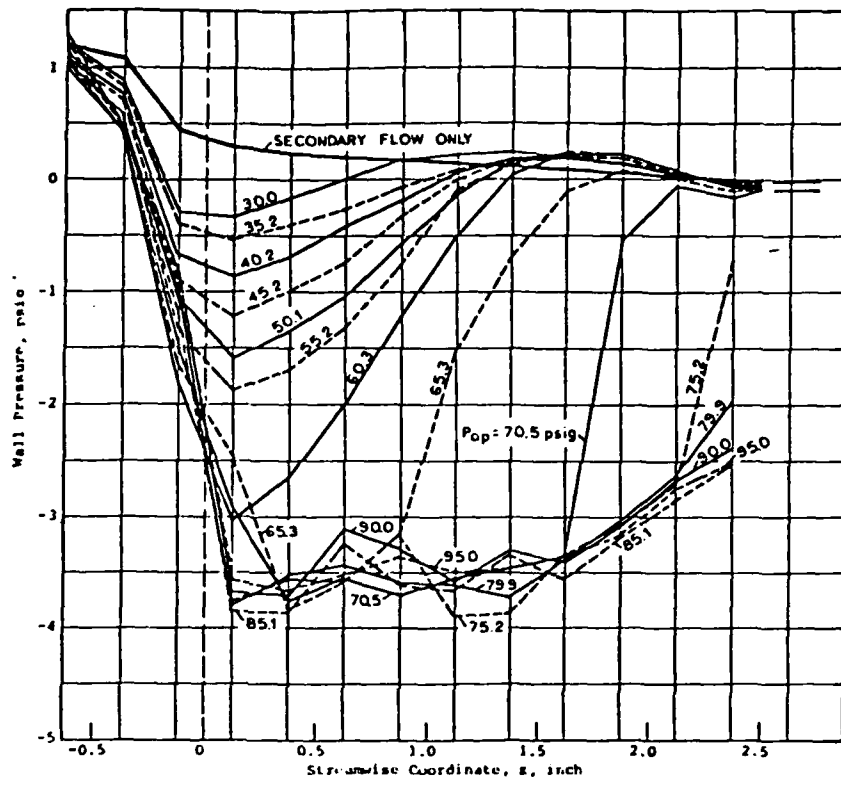


Figure 2

$a_s = 7.55$
 $M_\infty = 0.65$
 $(P_{\text{exit}} = 4.83 \text{ psig})$
 $X_2 = 0.250 \text{ inch}$
 $X_e = 0.250 \text{ inch}$
 $Z_m = 2.5 \text{ inch}$
Primary Nozzles:
 $\theta_p = 10^\circ$
 $x_p = -0.558 \text{ inch}$
 $x_p = 0.128 \text{ inch}$

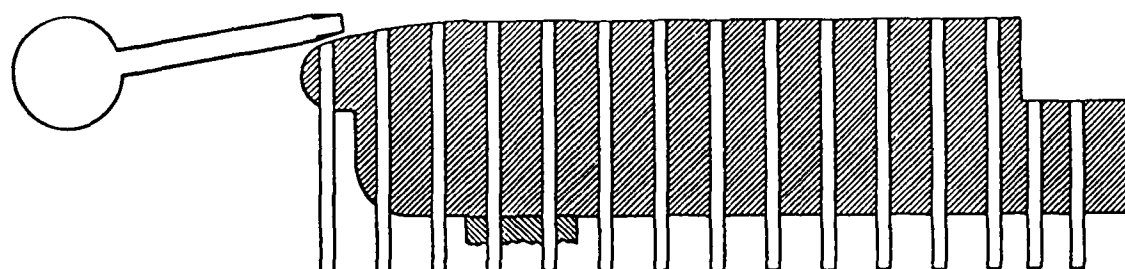
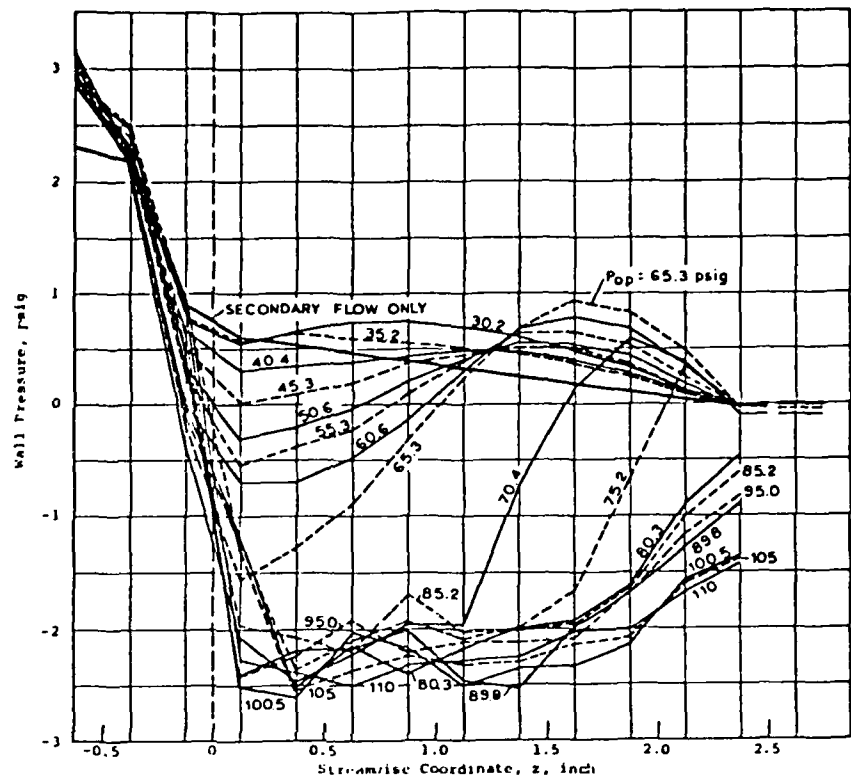


Figure 3

$a_s = 7.55$
 $M_\infty = 0.81$
 $(P_{\infty} = 7.93 \text{ psig})$
 $x_2 = 0.250 \text{ inch}$
 $x_d = 0.250 \text{ inch}$
 $z_m = 2.5 \text{ inch}$
Primary Nozzles:
 $\theta_p = 10^\circ$
 $x_p = -0.500 \text{ inch}$
 $x_p = 0.125 \text{ inch}$

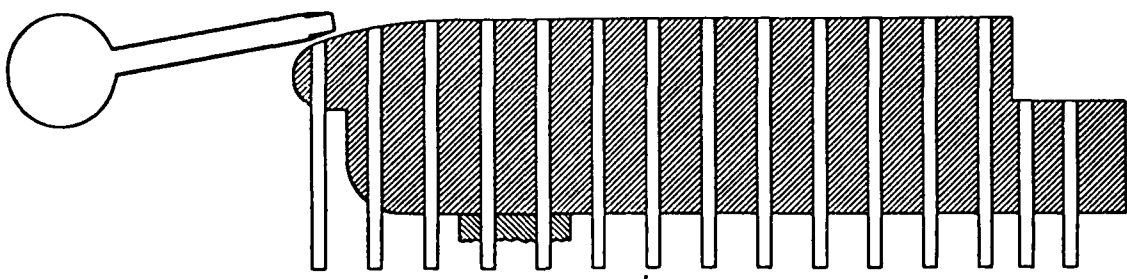
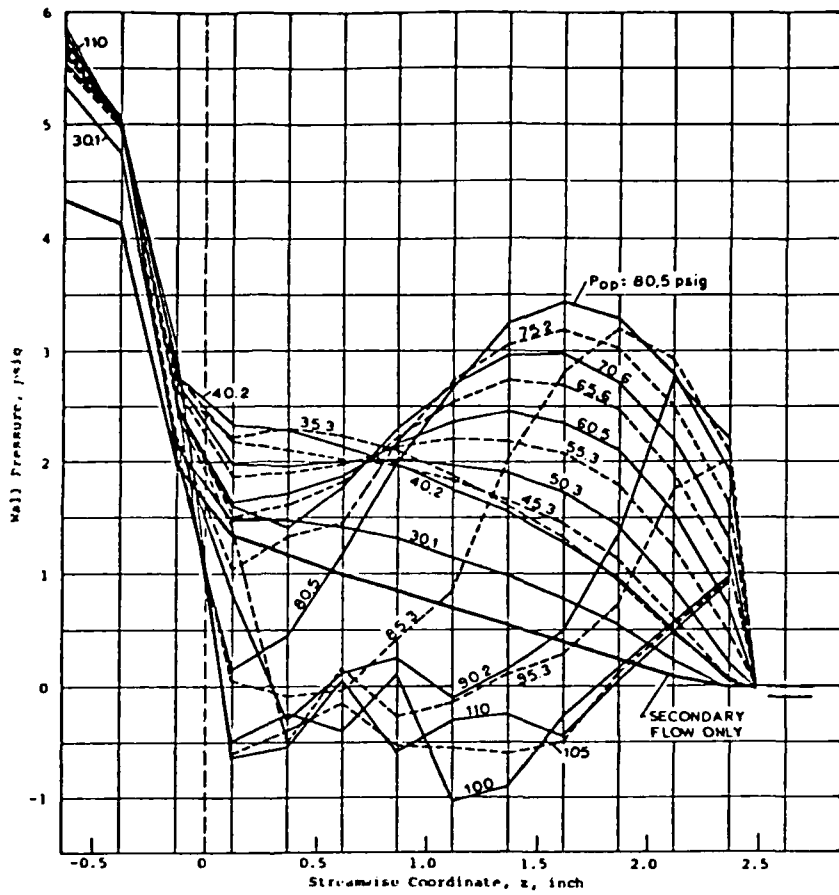


Figure 4

$a_s = 7.55$
 $M_m = 0.65$
 $(P_{\infty} = 4.83 \text{ psig})$
 $x_2 = 0.250 \text{ inch}$
 $x_e = 0.212 \text{ inch}$
 $z_m = 2.5 \text{ inch}$
Primary Nozzles:
 $\theta_p = 10^\circ$
 $x_p = -0.558 \text{ inch}$
 $x_{p'} = 0.128 \text{ inch}$

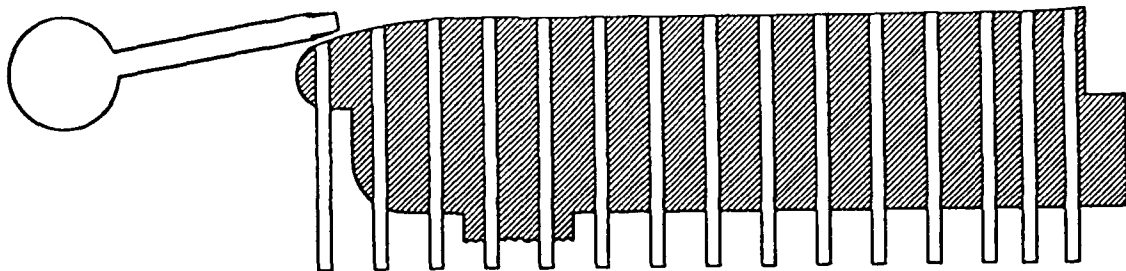
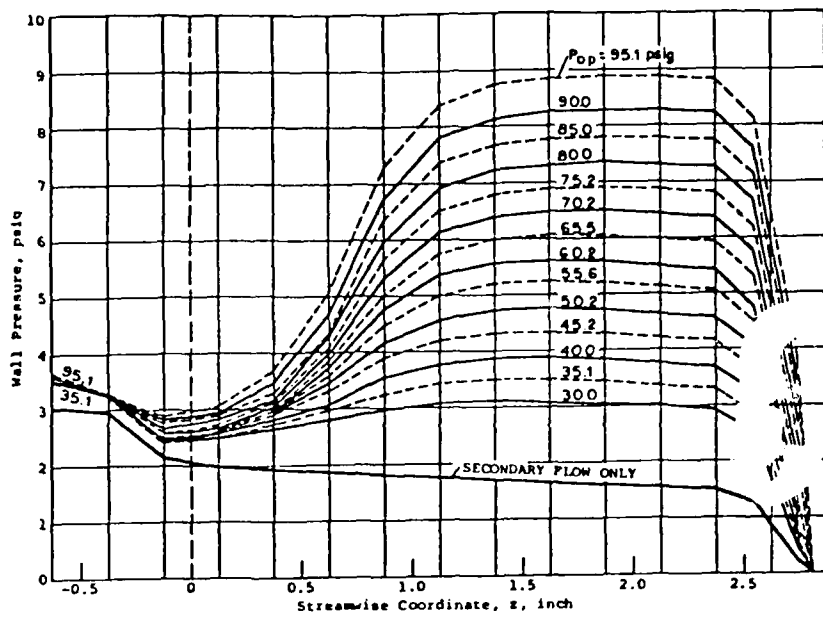


Figure 5

$a_s = 7.55$
 $M_\infty = 0.81$
 $(P_{\infty} = 7.93 \text{ psig})$
 $X_2 = 0.250 \text{ inch}$
 $X_e = 0.212 \text{ inch}$
 $Z_m = 2.5 \text{ inch}$
 Primary Nozzles:
 $\beta_p = 10^\circ$
 $z_p = -0.558 \text{ inch}$
 $x_p = 0.128 \text{ inch}$

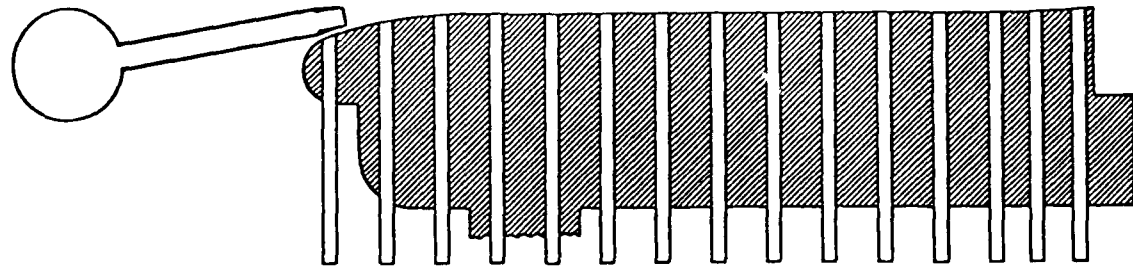
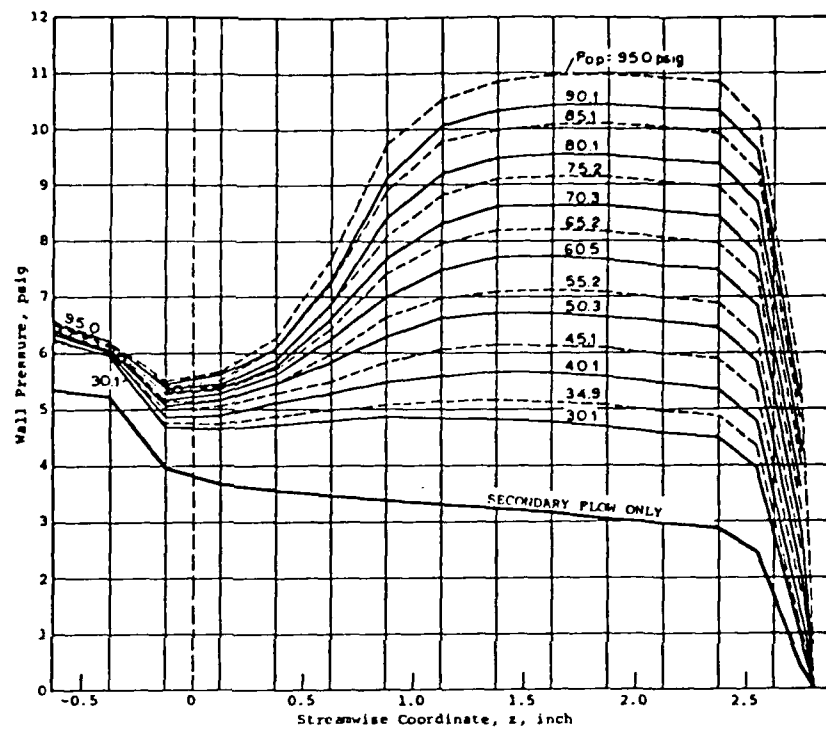


Figure 6

$\alpha_0 = 15.1$
 $M_\infty = 0.65$
 $(P_{O\infty} = 4.83 \text{ psig})$
 $x_2 = 0.501 \text{ inch}$
 $x_e = 0.443 \text{ inch}$
 $Z_m = 2.5 \text{ inch}$
 Primary Nozzles:
 $B_p = 10^\circ$
 $z_p = -0.565 \text{ inch}$
 $x_p = 0.209 \text{ inch}$

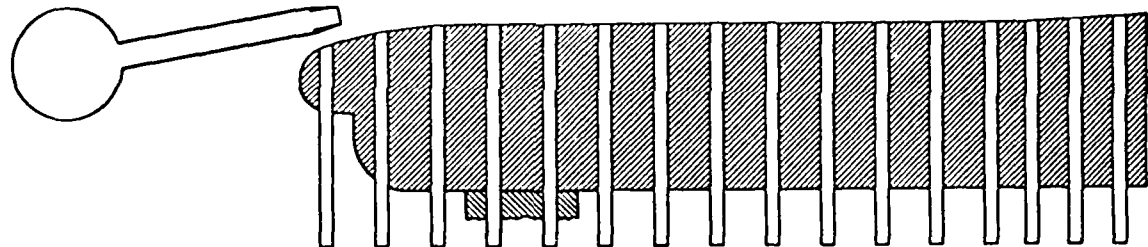
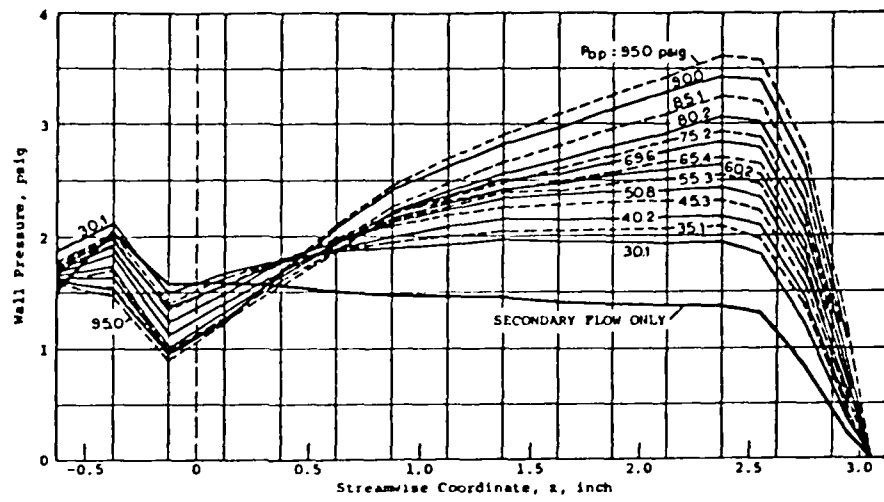


Figure 7

$\alpha_0 = 15.1$
 $M_\infty = 0.81$
 $(P_{\infty} = 7.93 \text{ psig})$
 $x_2 = 0.501 \text{ inch}$
 $x_0 = 0.443 \text{ inch}$
 $z_m = 2.5 \text{ inch}$
Primary Nozzles:
 $\beta_p = 10^\circ$
 $x_p = -0.565 \text{ inch}$
 $x_p = 0.209 \text{ inch}$

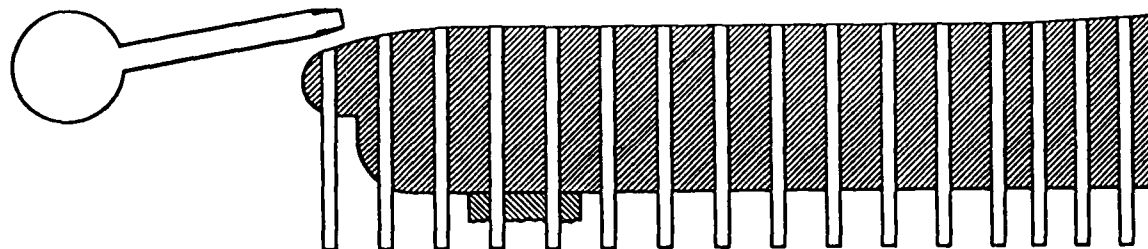
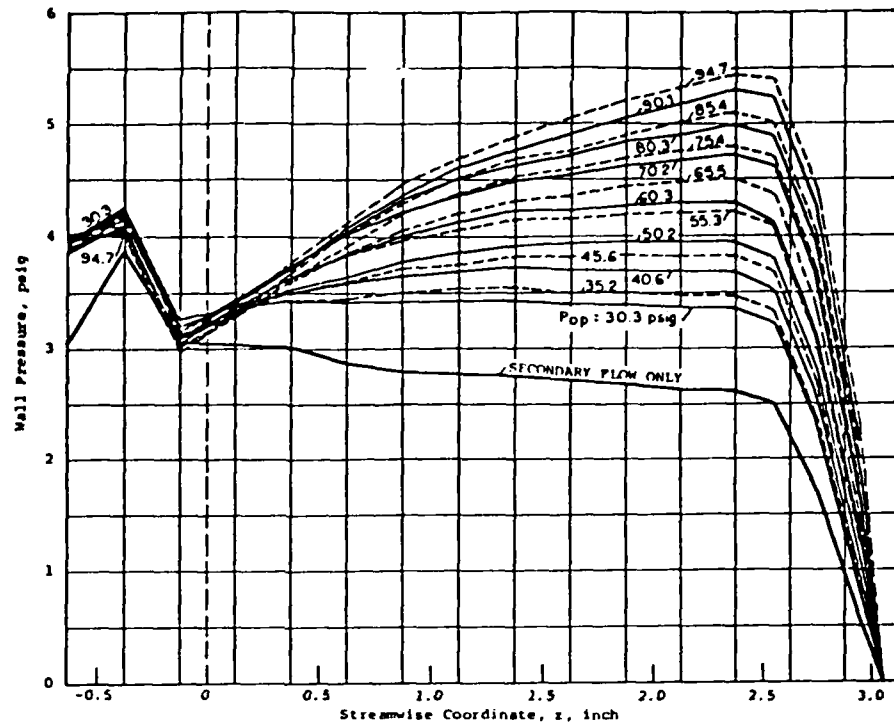
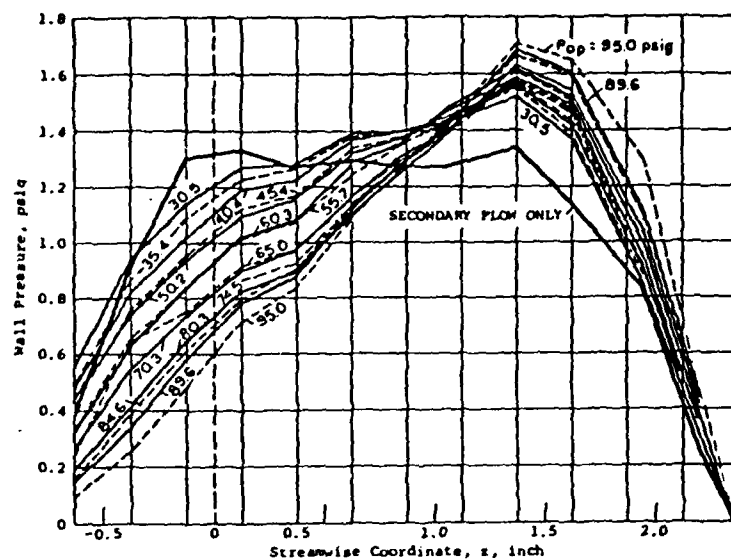


Figure 8

$u_e = 30.2$
 $M_e = 0.65$
($P_{\infty} = 4.83 \text{ psig}$)
 $x_2 = 0.986 \text{ inch}$
 $x_e = 0.883 \text{ inch}$
 $z_m = 1.5 \text{ inch}$
Primary Nozzles:
 $\beta_p = 0^\circ$
 $x_p = -0.463 \text{ inch}$
 $x_p = 0.350 \text{ inch}$



$D_o = 30.2$
 $H_o = 0.5$
 $(P_{O_m} = 2.74 \text{ psig})$
 $x_2 = 1.000 \text{ inch}$
 $x_e = 0.906 \text{ inch}$
 $z_n = 2.5 \text{ inch}$
 Primary Nozzles:
 $\beta_p = 8^\circ$
 $z_p = -0.463 \text{ inch}$
 $x_p = 0.350 \text{ inch}$

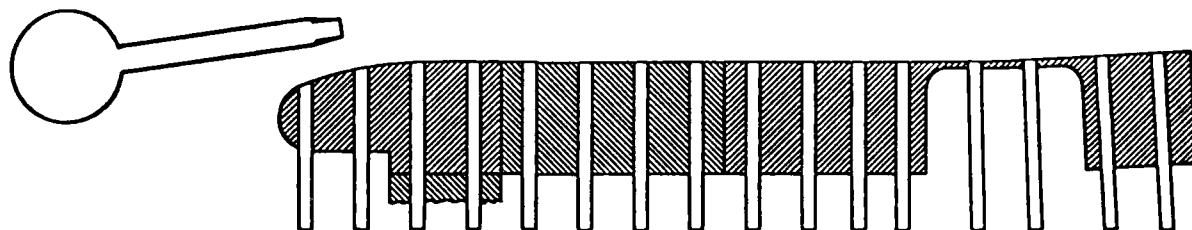
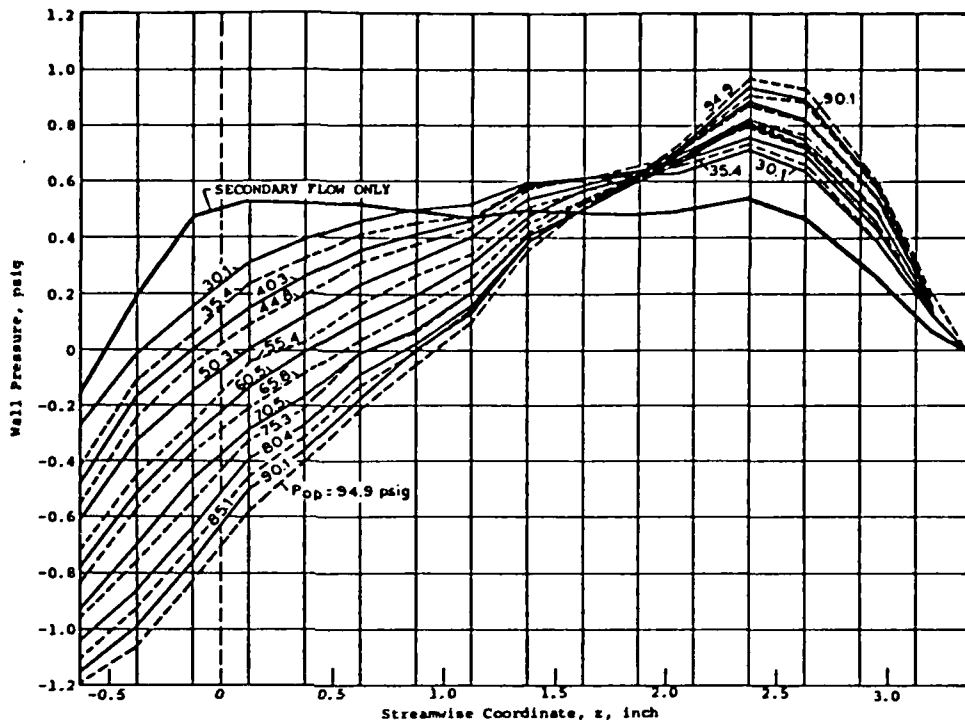
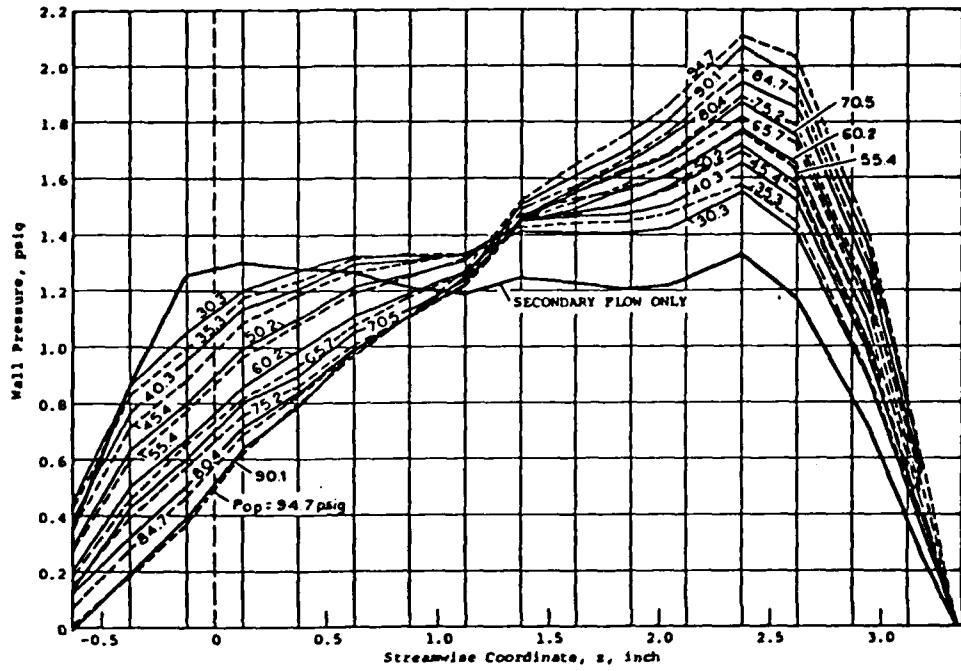


Figure 10

$a_s = 30.2$
 $M_m = 0.65$
 $(P_{\text{out}} = 4.83 \text{ psig})$
 $x_2 = 1.000 \text{ inch}$
 $x_0 = 0.906 \text{ inch}$
 $z_m = 2.5 \text{ inch}$
 Primary Nozzles:
 $\theta_p = 8^\circ$
 $x_p = -0.463 \text{ inch}$
 $x_p = 0.350 \text{ inch}$



$\alpha_0 = 30.2$
 $N_w = 0.81$
 $(P_{\text{atm}} = 7.93 \text{ psig})$
 $x_2 = 1.000 \text{ inch}$
 $x_0 = 0.906 \text{ inch}$
 $z_m = 2.5 \text{ inch}$
 Primary Nozzles:
 $B_p = 8^\circ$
 $x_p = -0.463 \text{ inch}$
 $x_p = 0.350 \text{ inch}$

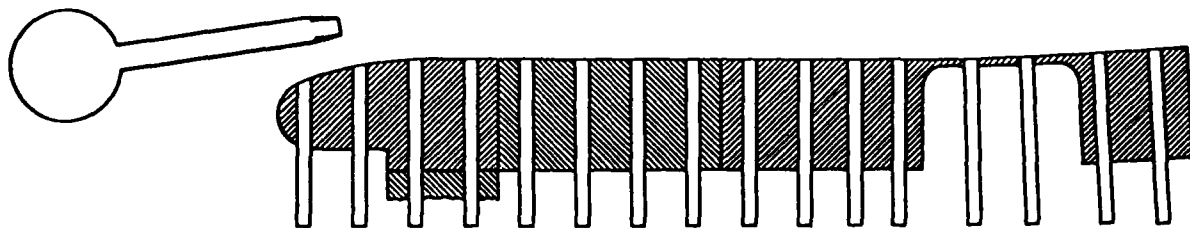
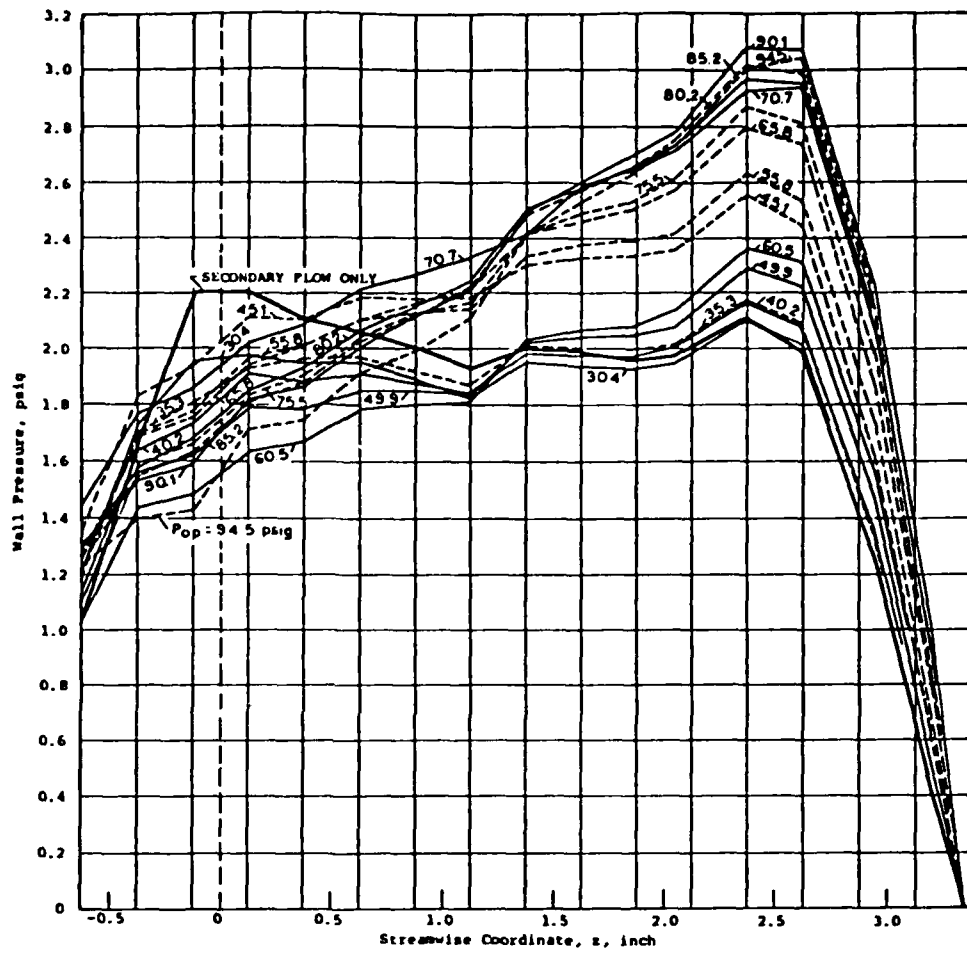


Figure 12

$U_\infty = 30.2$
 $M_\infty = 0.65$
 $(P_{\infty} = 4.83 \text{ psig})$
 $x_2 = 1.000 \text{ inch}$
 $x_e = 0.906 \text{ inch}$
 $z_e = 3.5 \text{ inch}$
Primary Nozzles:
 $B_p = 8^\circ$
 $s_p = -0.463 \text{ inch}$
 $x_p = 0.350 \text{ inch}$

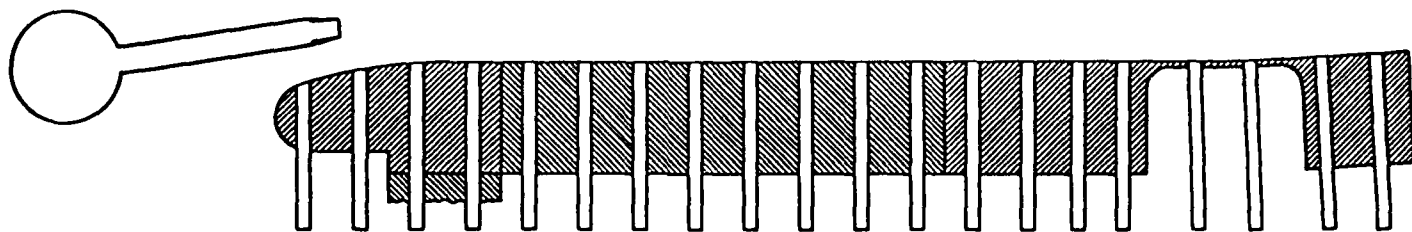
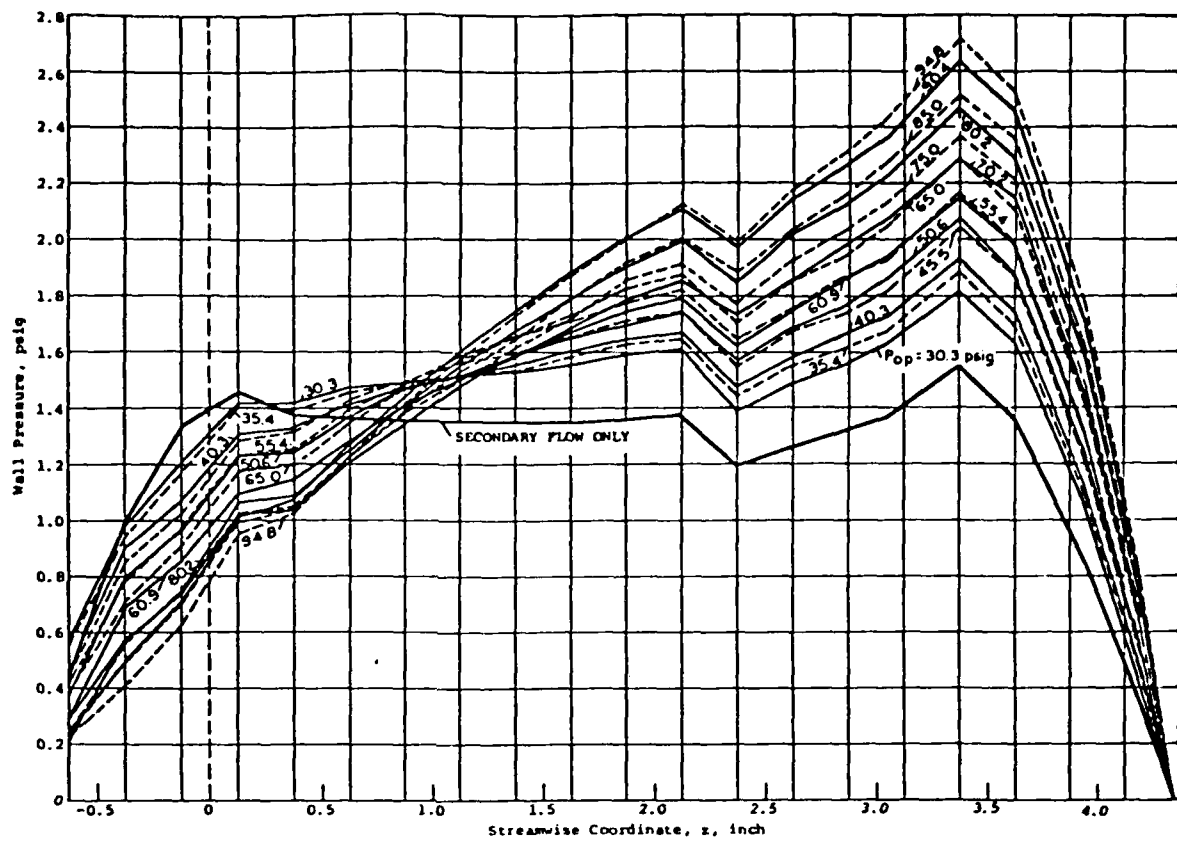


Figure 13

$\alpha_0 = 30.2$
 $M_\infty = 0.81$
($P_{\text{atm}} = 7.93 \text{ psig}$)
 $x_2 = 1.000 \text{ inch}$
 $x_e = 0.906 \text{ inch}$
 $z = 3.5 \text{ inch}$
Primary Nozzles:
 $\theta_p = 8^\circ$
 $s_p = -0.463 \text{ inch}$
 $x_p = 0.350 \text{ inch}$

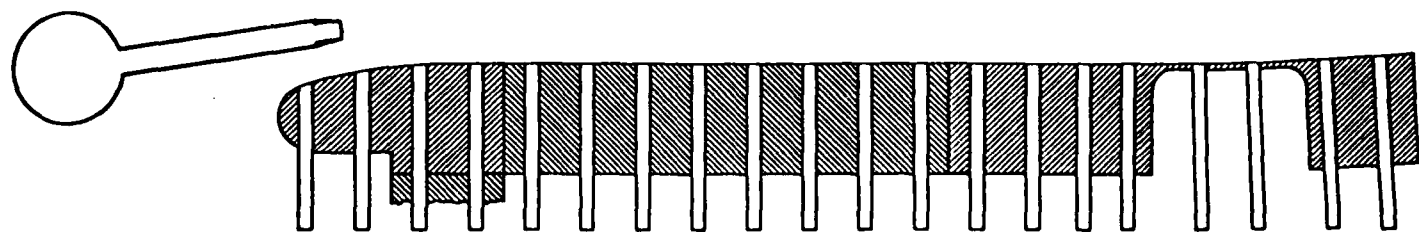
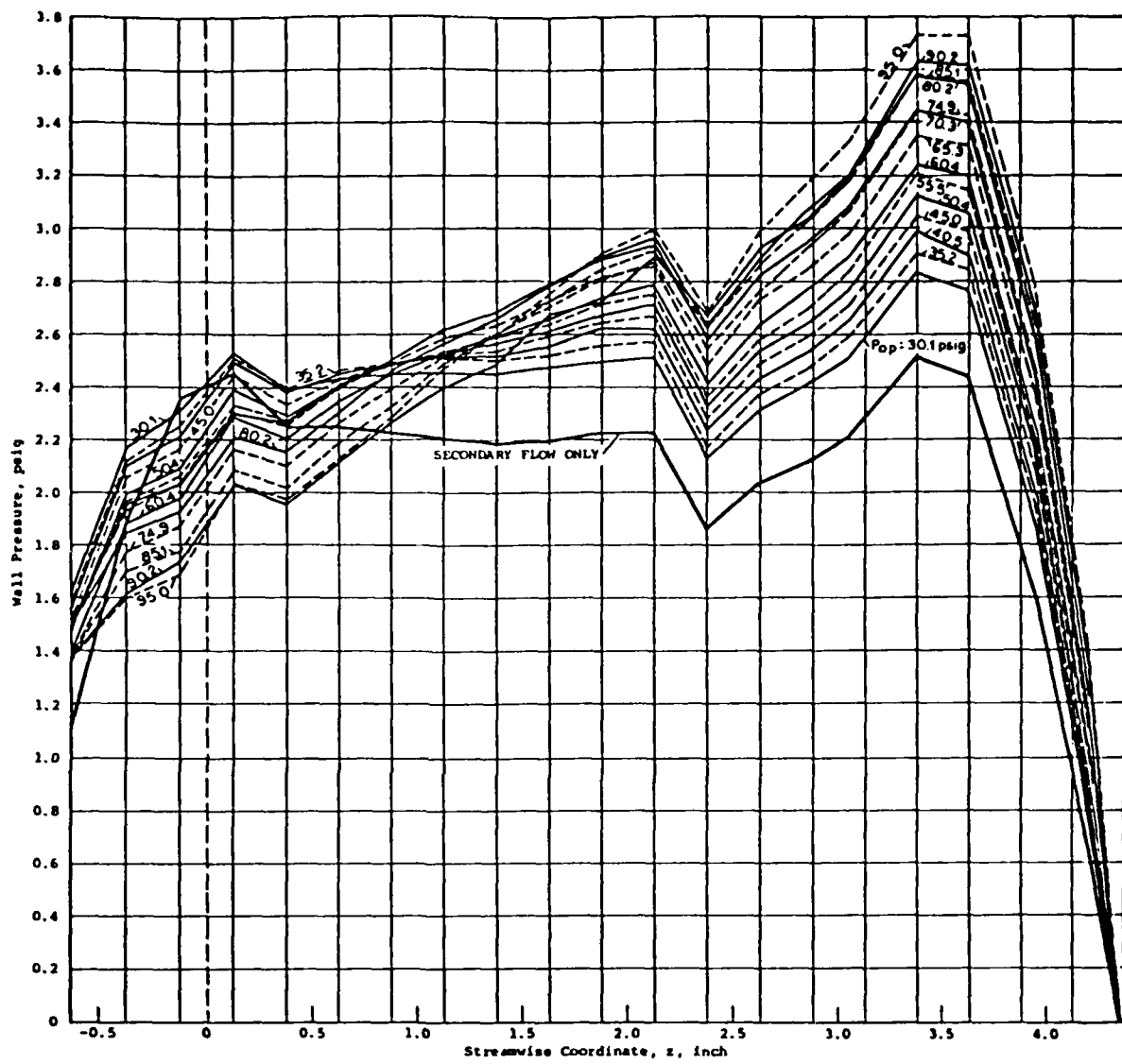


Figure 14

$a_0 = 15.1$
 $M_\infty = 0.65$
 $(P_{\infty} = 4.83 \text{ psig})$
 $x_2 = 0.250 \text{ inch}$
 $x_3 = 0.220 \text{ inch}$
 $z_0 = 2.5 \text{ inch}$
 Primary Nozzle:
 (Single Central)
 $x_p = -0.25 \text{ inch}$

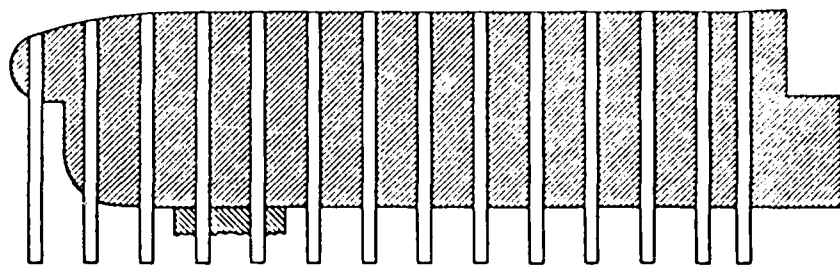
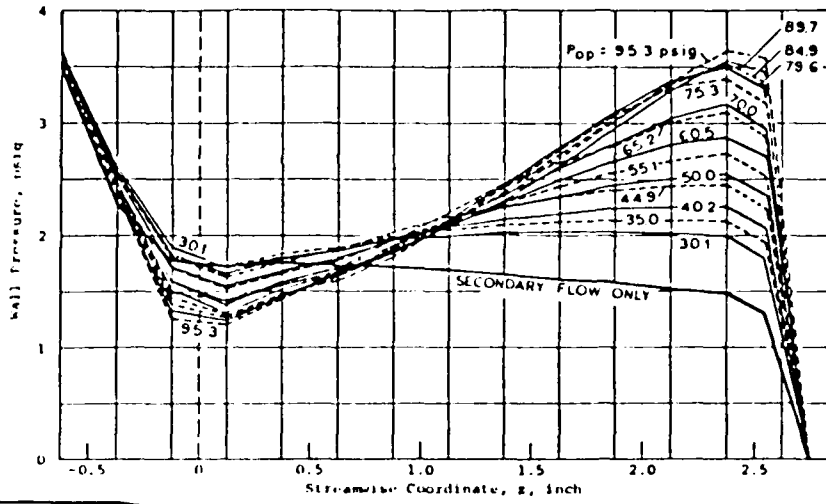
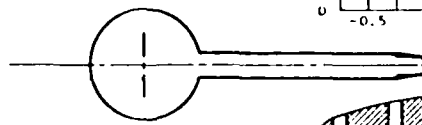


Figure 15

$D_o = 15.1$
 $M_\infty = 0.81$
 $(P_{1\infty} = 7.93 \text{ psig})$
 $X_2 = 0.250 \text{ inch}$
 $X_e = 0.220 \text{ inch}$
 $Z_m = 2.5 \text{ inch}$
 Primary Nozzle
 (Single Central)
 $x_p = -0.25 \text{ inch}$

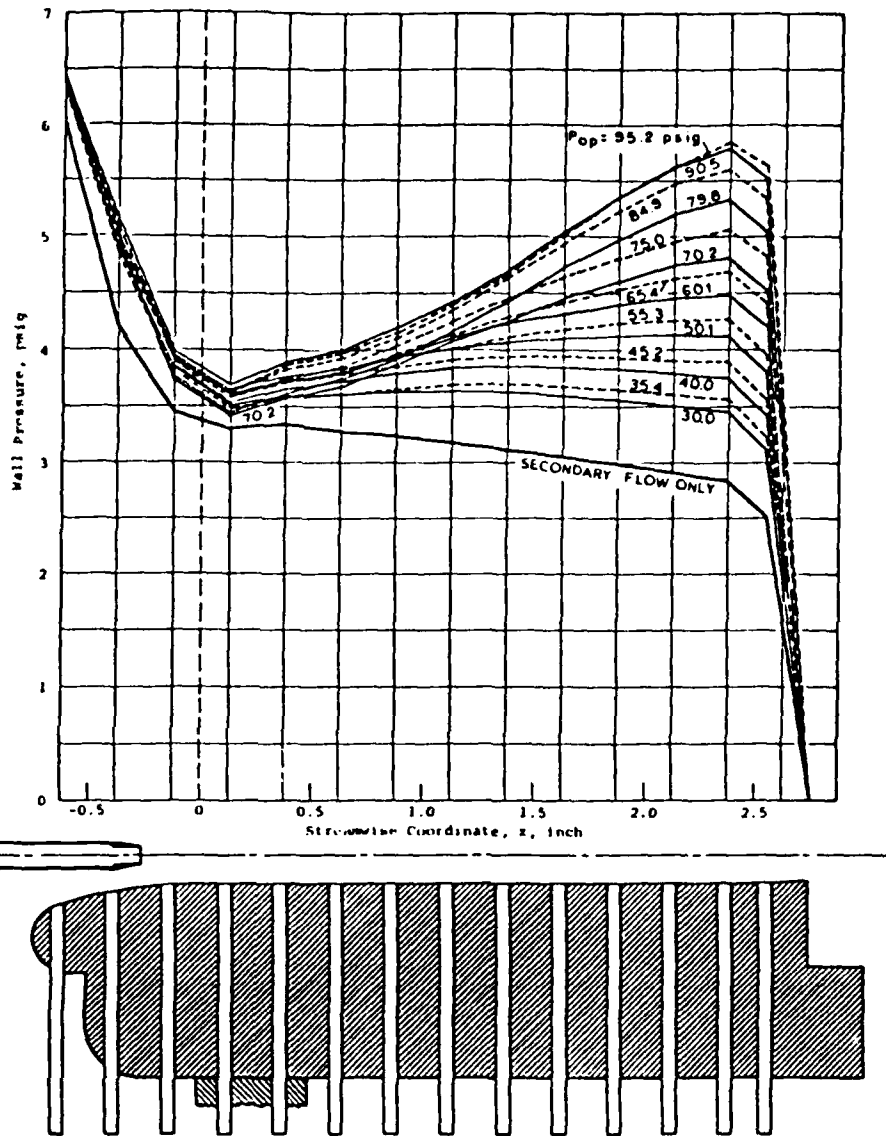


Figure 16

$a_s = 15.1$
 $n_m = 0.81$
 $(P_{\text{out}} = 7.93 \text{ psig})$
 $x_2 = 0.250 \text{ inch}$
 $x_e = 0.220 \text{ inch}$
 $z_m = 2.5 \text{ inch}$
 Primary Nozzle
 (Single Central)
 $z_p = -0.75 \text{ inch}$

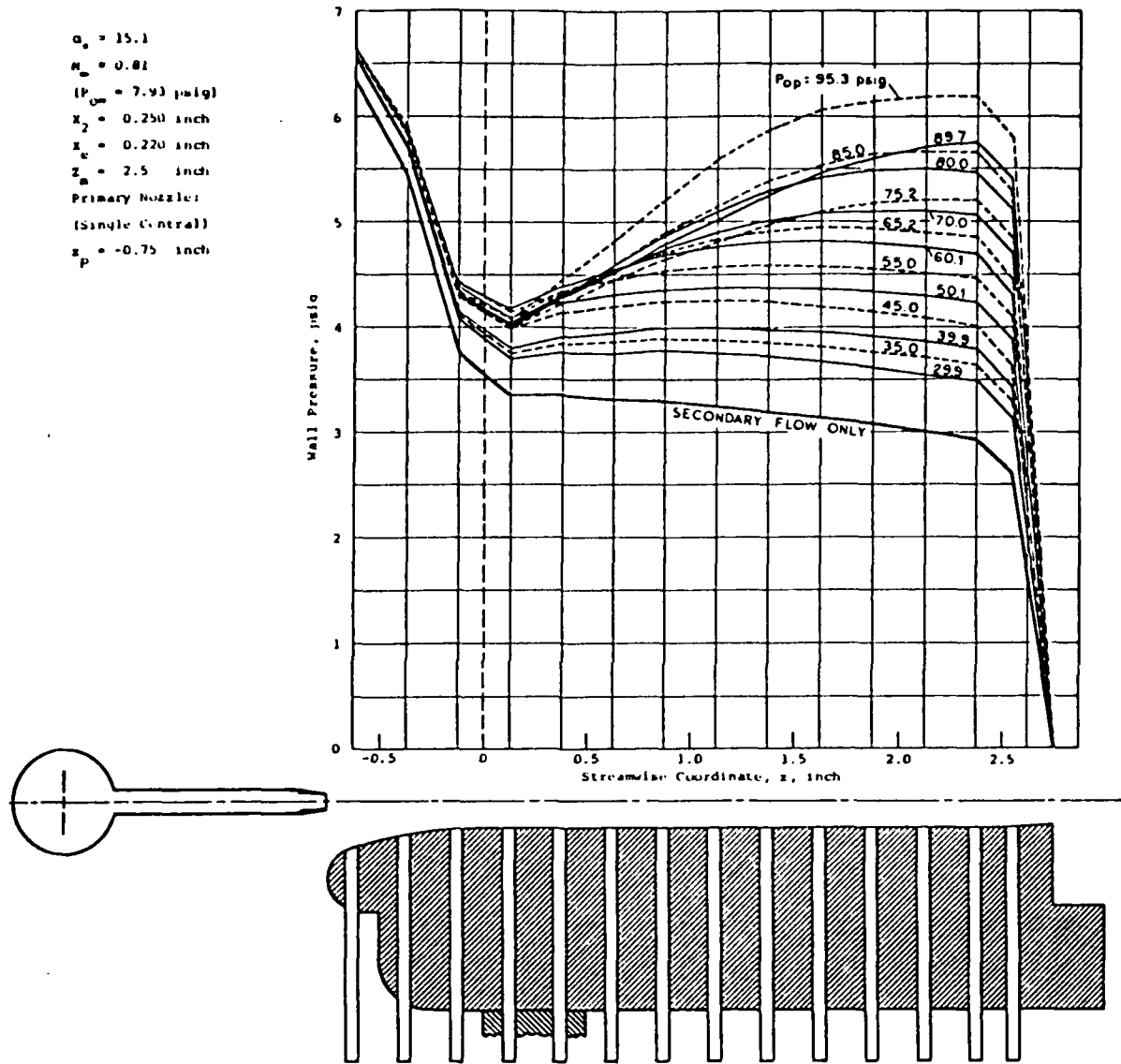


Figure 17

$\alpha_0 = 30.2$
 $M_0 = 0.65$
 $(P_{C_\infty} = 4.83 \text{ psig})$
 $x_2 = 0.501 \text{ inch}$
 $x_0 = 0.440 \text{ inch}$
 $z_0 = 2.5 \text{ inch}$
 $a_0 = -0.25 \text{ inch}$
Primary Nozzle:
 (Single Central)
 $x_p = -0.25 \text{ inch}$

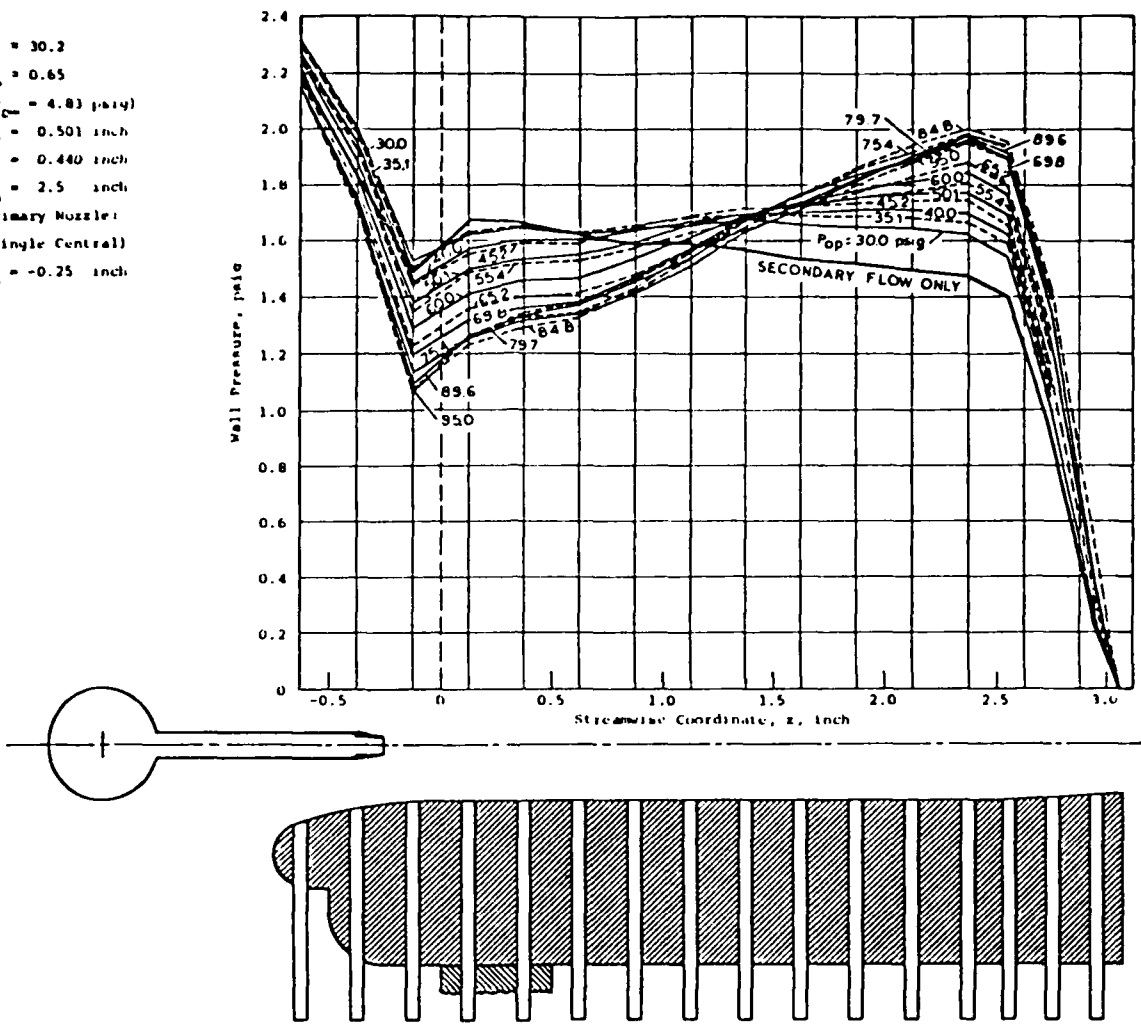


Figure 18

$a_s \approx 30.2$
 $M_\infty = 0.5$
 $P_{op}/P_\infty = 6.1$

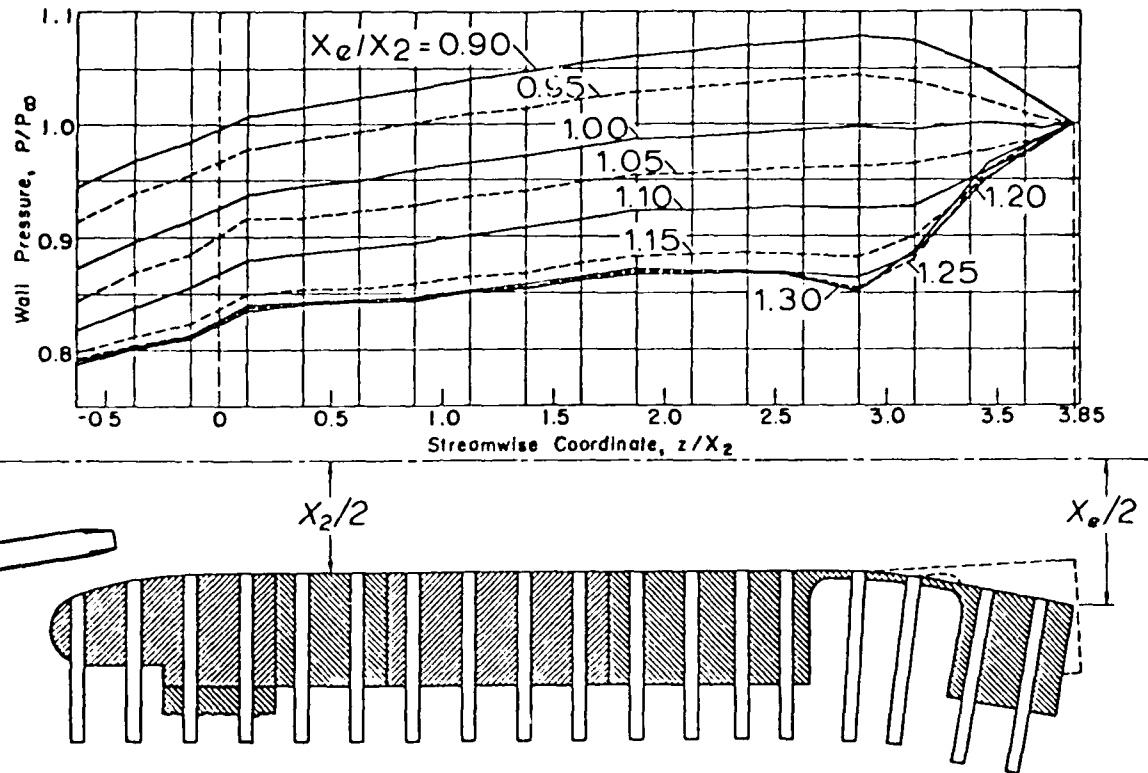


Figure 19

$\alpha_s \approx 30.2$
 $M_\infty \approx 0.65$
 $P_{op}/P_\infty = 6.1$

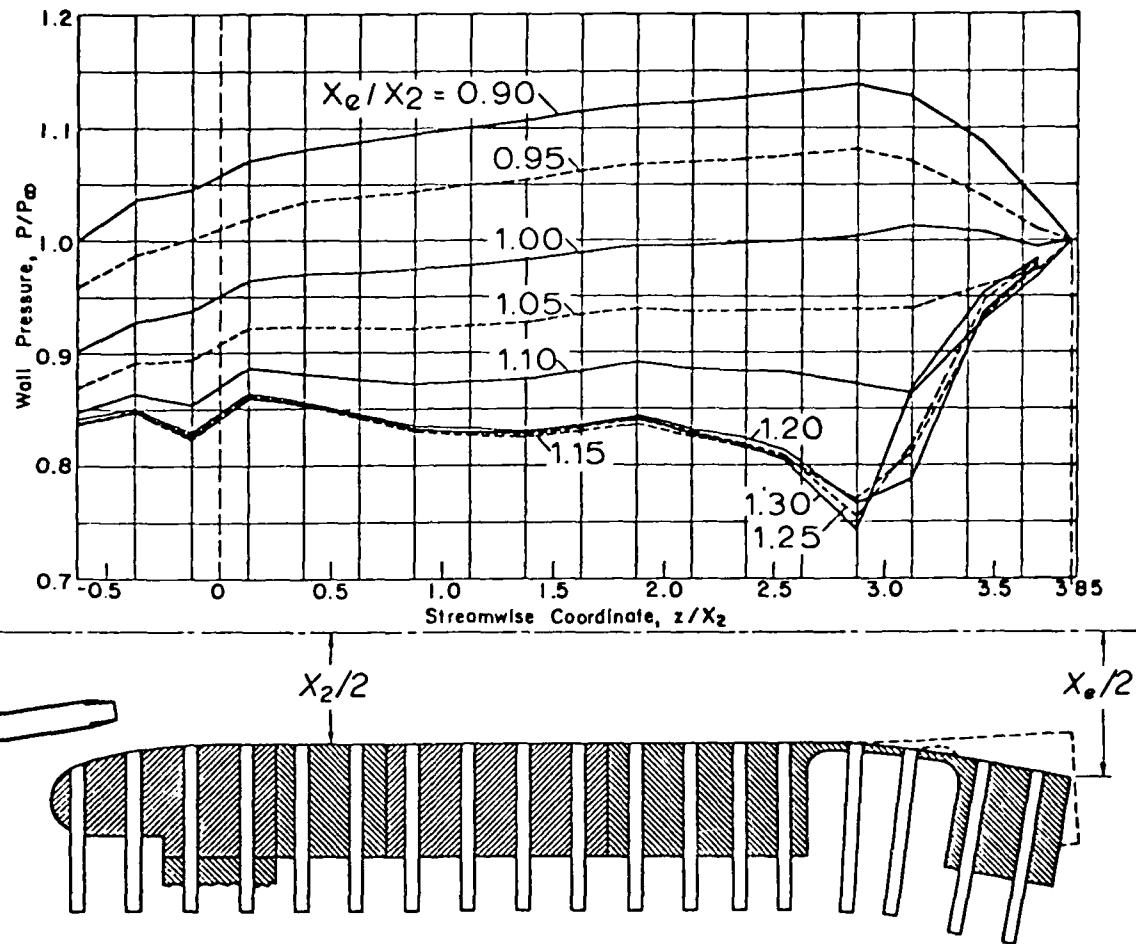


Figure 20

$\alpha_* \approx 30.2$
 $M_\infty \approx 0.81$
 $P_{op}/P_\infty = 6.1$

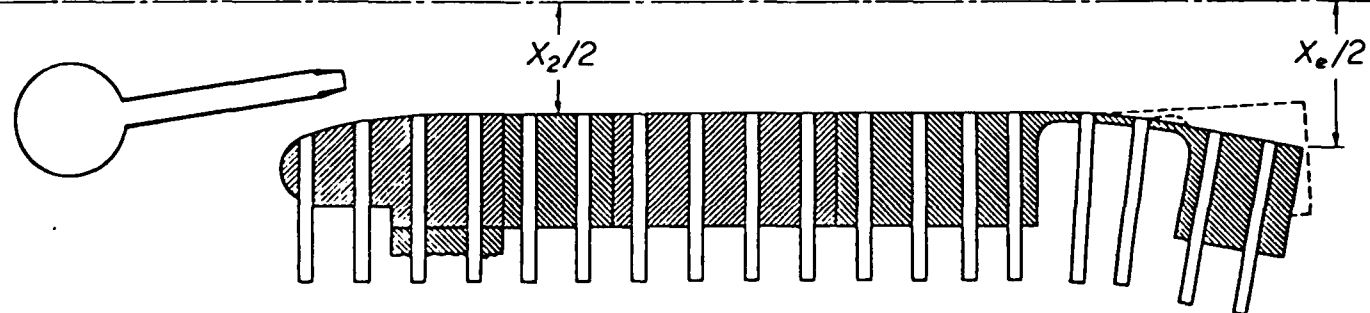
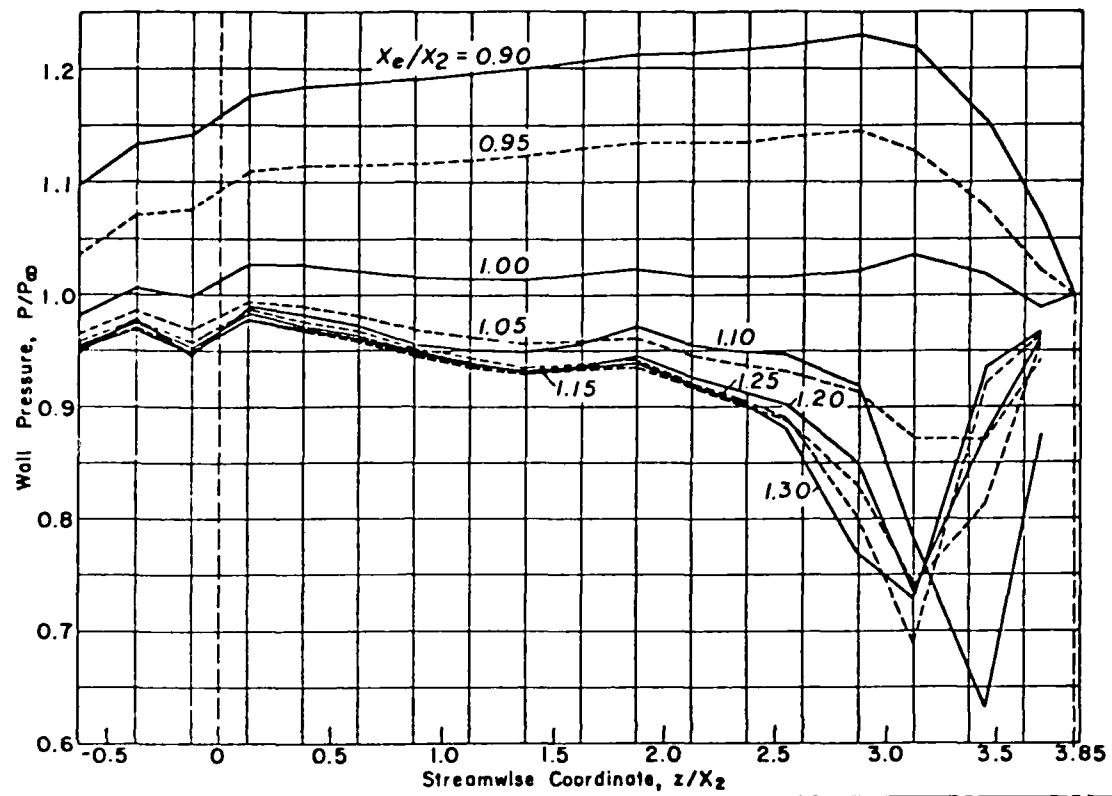
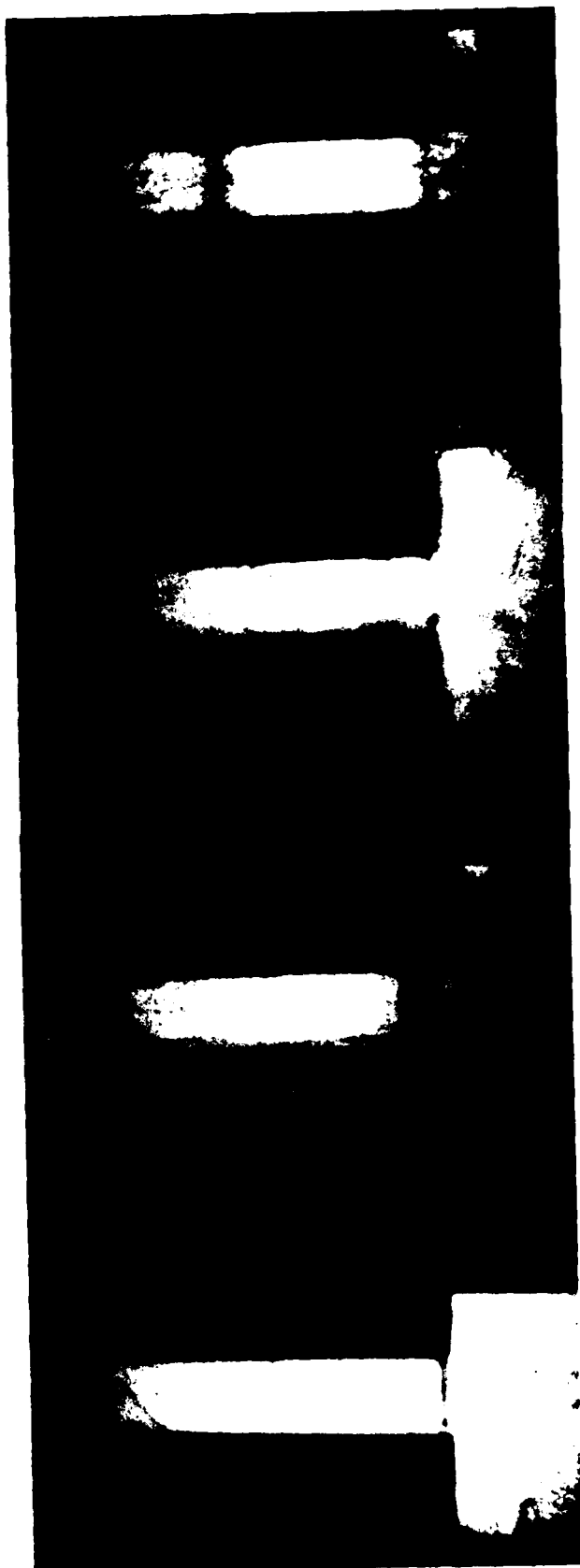


Figure 21

$P_{op} = 70.5 \text{ psig}$



$P_{op} = 75.2 \text{ psig}$

$P_{op} = 79.9 \text{ psig}$

$P_{op} = 85.1 \text{ psig}$

Figure 22. Formation of Starting
Shock Wave
 $M_\infty = 0.5; \alpha_* = 7.55$

Examples of Ejector Flows under the Second Solution

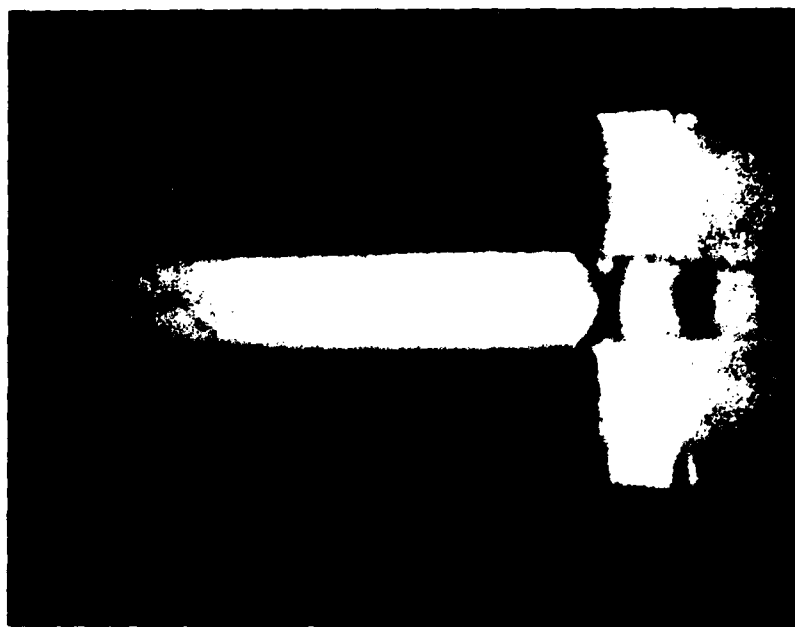


Figure 23. $M_\infty = 0.65$, $\alpha_* = 7.55$, $x_2 = x_e = 0.25"$, $z_m = 2.5"$, $p_{op} = 105$ psig

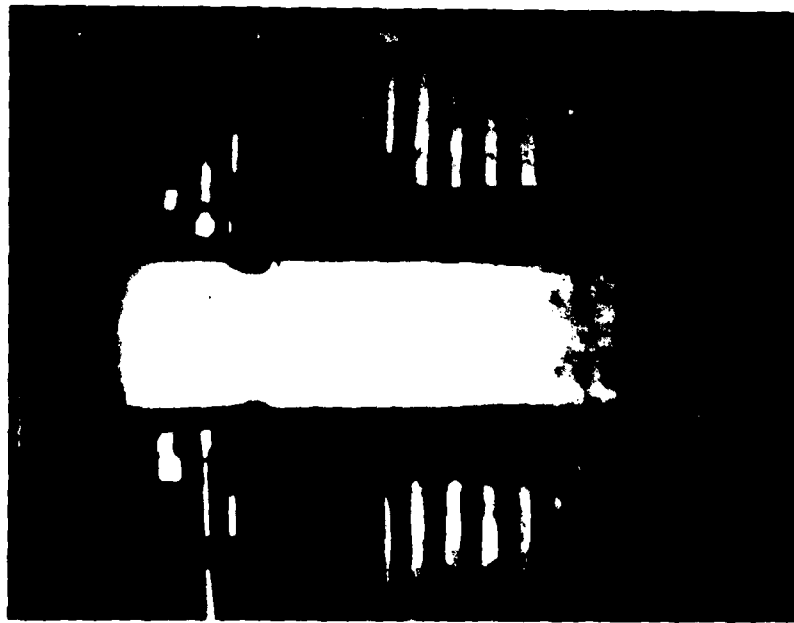


Figure 24. $M_\infty = 0.81$, $\alpha_* = 30.2$, $x_2 = 1"$, $x_e = 1.1"$, $z_m = 3"$, $p_{op} = 75$ psig